



Optimization of membrane structure using the spin-coating method

Zhenghui Wang, Jun Ma*, Panpan Wang

*Harbin Institute of Technology, State Key Laboratory of Urban Water Resource and Environment, National Engineering Research Center of Urban Water Resources, Harbin 150090, PR China
Tel. +86 451 86282292; Fax: +86 451 82368074; email: majun@hit.edu.cn*

Received 3 September 2010; Accepted 3 January 2011

ABSTRACT

Spin-coating is a preferred method for application of thin and uniform films on flat substrates, it is used extensively in microlithography. For polymeric membranes prepared by the immersion-precipitation method, the solvent-nonsolvent mass transfer kinetics always governs the ultimate membrane structure to a large extent. In this paper, the effects of spinning conditions on the mass transfer kinetics and thus the structure and performance of very thin and smooth membranes were investigated. The results indicated that the membrane structures can be regulated in a relatively large range through adjusting the spinning conditions (spinning speed, spinning time, acceleration process). With proper control, formation of membranes with round-pore surfaces or nodular surfaces can be achieved.

Keywords: Polymeric membrane; Structure; Film; Casting solution; Spin-coating; Mass transfer kinetics

1. Introduction

Precise control on the pore structure of membrane is always highly valued, so far, various methods have been tried to achieve that [1–5]. Smolders et al. made a comprehensive study on the formation of phase inversion membranes, the effects of factors including the selection of polymer, solvent, non-solvent, additive, evaporation and coagulation condition were investigated, relevant mechanisms were proposed [6–9]. Yan et al. prepared the porous membranes with very narrow pore size distribution using pillar arrays as templates [2]. Kshama et al. fabricated nanotubule-based molecular-filtration membranes with excellent selectivity through depositing nano-Au particles on the pore walls of track-etched polycarbonate membranes [5]. Park and other researchers' work indicated that self-assembly of block copolymers would be an effective means to generate membranes with ordered structure [10,11].

Though above literature review indicates that there may be many potential solutions of realizing fine-tune on membrane pore structure, the traditional phase inversion method especially the immersion-precipitation type still plays a main role in preparing the practically used membranes today. Due to that, many current researches still focus on this method and try to better understand its mechanism [12–14], however, most of the membranes in those works are casted using a knife-like tool to disperse the polymer solution and control the thickness of the nascent membrane. In contrary, spin-coating is much better in applying thin and uniform films on flat substrates, thus makes it possible to further advance the study on formation of membrane structure [14–17].

In the present work, the effects of spinning speed and time on the morphology (surface, cross-section, thickness), permeability, and rejection property of the membranes were investigated, the structure-property relationship were analyzed. The results showed that some special pore structures can be generated through proper controlling the spinning process.

*Corresponding author.

2. Experimental

2.1. Materials

Poly(vinylidene fluoride), obtained from Shanghai 3F New Materials Co., Ltd. (FR904, $M_n = 475,637$) was used as the membrane material. Dimethylacetamide (DMAc, Tianjin Bodi Chemicals Co., Ltd. >99%, Analytical reagent) and distilled water were used as the solvent and nonsolvent, respectively. Poly(vinylpyrrolidone) (PVP K30, Beijing Pinghao Biotechnology Co., Ltd. Analytical reagent) was used as the polymeric additive. Pepsin ($M_w = 35,000$ g/mol) used in the rejection test was purchased from DongWu Bio-Chemical Products Company in Su Zhou. All the materials were used as received.

2.2. Membrane preparation

Membranes were prepared through first spin-coating a liquid dope solution layer on a glass plate and then coagulating them into the nonsolvent bath.

Proper weight of PVDF (18 wt%) and PVP (2 wt%) were added into DMAc (80 wt%), the mixtures were vigorously stirred for 10 h under 60°C to ensure a complete dissolution. Then the solutions were placed in sealed bottles and degassed for 36 h. After that, the homogeneous solutions were spin-coated on circle glass plates with a spin-coater (KW-4A, Xia Men Chemat scientific instruments Co., Ltd.) at different spinning conditions (Relevant parameters in detail will be given in Section 3). After coating (Relative humidity ranged from 46% to 50%), the nascent membranes (together with the substrates) were immediately immersed into distilled water (25°C). The subsequently detached films were moved into another distilled water container and kept for 3 d. Then certain areas of each membrane were taken out and subjected to permeability and rejection test, the left membranes were immersed into ethanol for 12 h, after that the membranes were dried in air and the dry samples would undergo structure examination.

2.3. Membrane characterization

2.3.1. Scanning electron microscopy (SEM) analysis

To observe the cross-section structures of the membranes, the dry samples were immersed into liquid nitrogen and fractured carefully which would give a clean break, then all the specimens were fixed on a metal support and sputtered a layer of gold under vacuum with proper thickness. After that, the membrane structures were examined using a scanning electron microscope (SEM, Phillip's SEM model FEI. Sirion 200, Netherlands).

2.3.2. Permeability test

Permeability (pure water flux) of membrane was measured using a membrane testing unit (Shanghai Mosu Scientific Equipment Co., Ltd, China). The obtained membrane sheets were cut into circles of 31.5 mm in diameter and subsequently were installed into the testing unit. Firstly, the trans-membrane pressure was set at 0.2 MPa (supplied by nitrogen gas), after 20 min of distilled water permeation the flux was practically constant, then the trans-membrane pressure was restored to 0.1 MPa after which one minute's permeate was collected to calculate the pure water flux.

2.3.3. Rejection measurement

For one piece of membrane sample, after the measurement of pure water flux, pepsin solution (200 ppm) was fed into the testing unit, the feed solution was stirred at about 360 r/min. A certain amount of permeate was collected under 0.1 MPa. The percentage rejection (R) can be calculated according to the formula:

$$R = 1 - C_p / C_f \quad (1)$$

where C_f and C_p denote the pepsin concentration in feed and permeate, respectively. Pepsin concentration was determined by a UV-visible spectrophotometer (UV-2550, Shimadzu) at 280 nm (In this paper, each reported flux and rejection value was expressed by the average of three sample measurements for each casting condition).

3. Results and discussion

3.1. Effect of spinning time on membrane structure

Surface and cross-section structures of the membranes prepared with different spinning time were shown in Fig. 1 and 2, respectively.

Fig. 1 showed that the membrane surfaces (a and b) were dense at relatively short spinning time. With the increase of spinning time, visible pores gradually appeared on membrane surface (c and d). Fig. 2(a) and (b) displayed the suppression of the typical macrovoid structures as the spinning time increased. While in Fig. 2(c) and (d), the macrovoid structures became some disordered, especially in Fig. 2(d), the walls of those voids broke, the alignment of them disappeared. Moreover, it can be found in Fig. 2 that the thickness of these membranes gradually decreased.

During the spinning process, two physical changes would occur to the initially deposited polymer solution. One is the thinning of coating layer, the other is the evaporation of solvent (DMAc). Thus, as the spinning time increased, the nascent membrane layer would

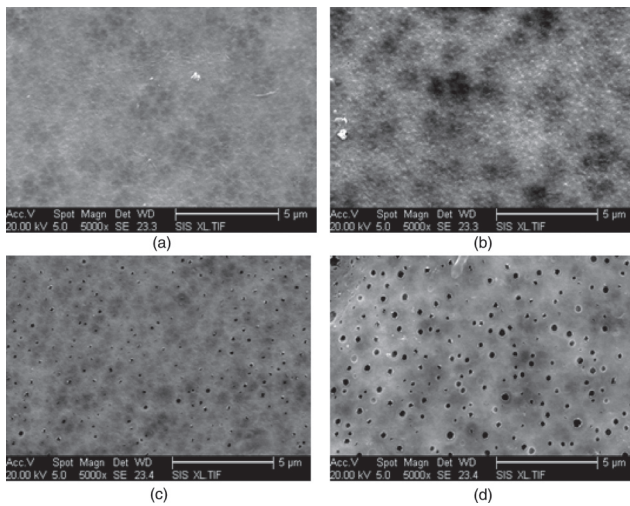


Fig. 1. Surface structures of the membranes prepared with different spinning time (spinning speed 3000 r/min): (a) 60s, (b) 120s, (c) 180s, (d) 240s.

become thinner, meanwhile, polymer content of the layer would increase which would accordingly increase the layer's viscosity. The gradual thinning of layer thickness and concentration of polymer solution tend to cause the suppression of the macrovoid structure (Fig. 2(a) and (b)) in the subsequent immersion-precipitation process [7]. However, it is still not clear why, at longer spinning time, the membrane cross-sections became disordered (Fig. 2(a) and (b)) but not change into sponge-like and why the membrane surfaces became

more and more porous? The possible answers to these two questions are given below.

Since solvent would evaporate from the solution layer, thus, the longer the spinning time, the more the solvent lost. On one hand, the increase of layer viscosity caused by solvent evaporation would slow further evaporation of solvent. On the other hand, when the polymer concentration increased to a certain value, the layer would become thermodynamically unstable, further decrease of solvent content would lead to phase separation in the layer [1,7,13]. Fig. 2(c) and (d) suggested that the evaporation induced phase separation had happened before the end of the spinning process. Especially in Fig. 2(d), it is thought that those disordered lattice-like structures and macrovoids on membrane cross-section were the composite result of evaporation induced phase separation and the afterward nonsolvent induced phase separation. Obviously, formation of those visible pores on membrane surface (Fig. 1(c) and (d)) should have a certain relation with the evaporation induced phase separation though more specific mechanism is not clear by now [18,19].

3.2. Effect of spinning speed on membrane structure

Surface and cross-section structures of the membranes prepared with different spinning speed were shown in Fig. 3 and 4, respectively.

Fig. 3 and 4 showed that, with the increase of spinning speed, surface of the membranes became more porous and cross-section of the membranes became

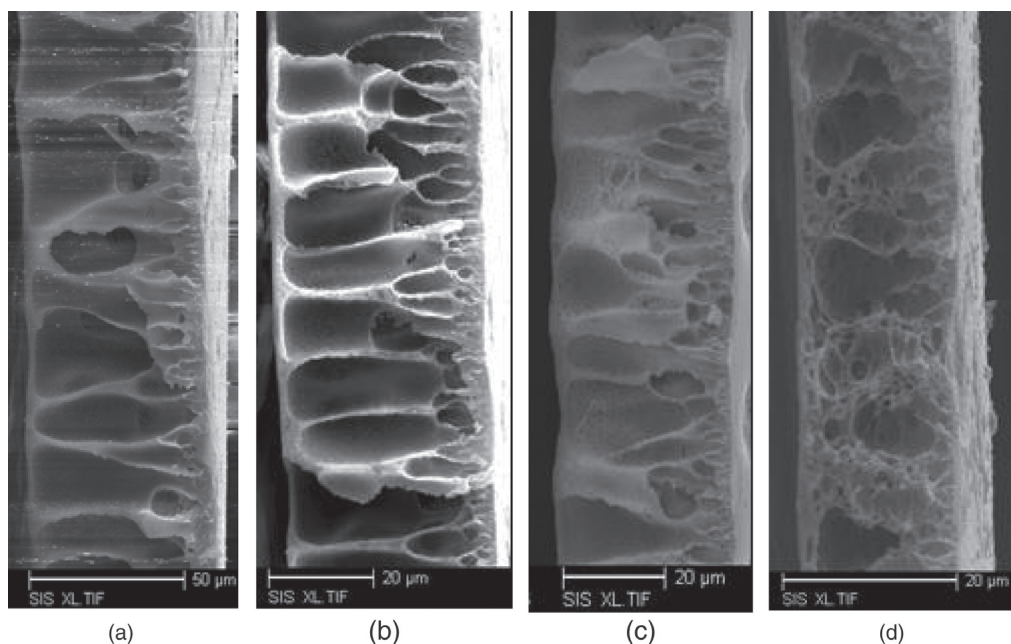


Fig. 2. Cross-section structures of the four membranes shown in Fig. 1.

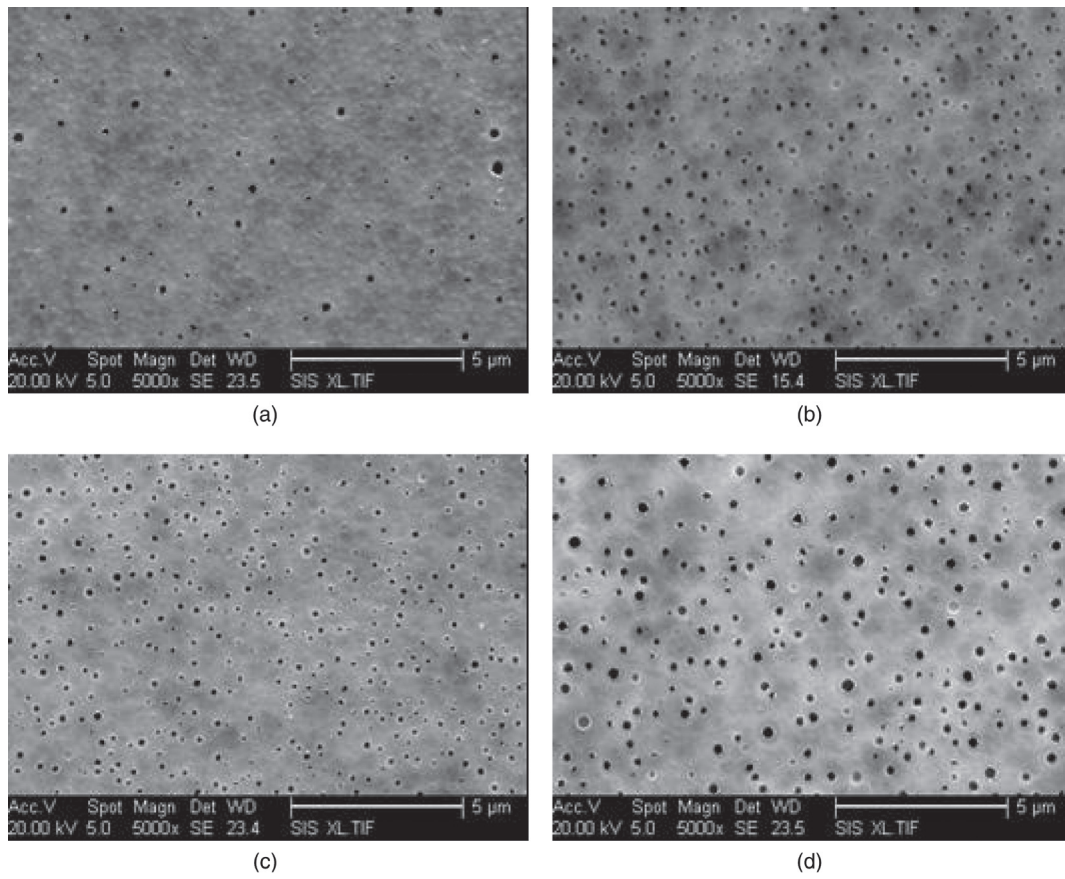


Fig. 3. Surface structures of the membranes prepared with different spinning speed (spinning time 120s): (a) 4000 r/m, (b) 6000 r/m, (c) 7000 r/m, (d) 9000 r/m.

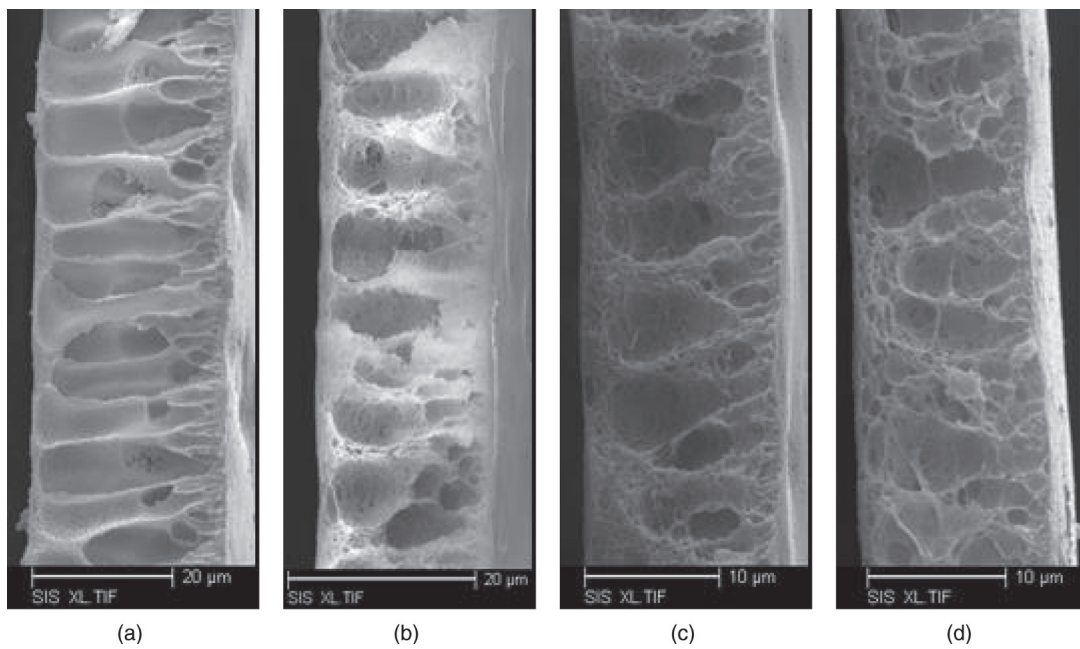


Fig. 4. Cross-section structures of the four membranes Fig. 3.

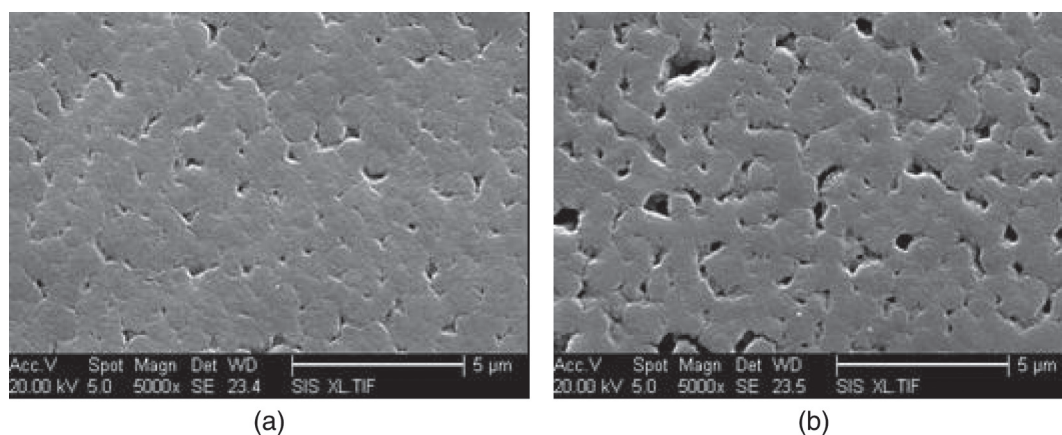


Fig. 5. Surface structures of two membranes prepared with high spinning speed and long spinning time: (a) 7000 r/m-180s, (b) 9000 r/m-240s.

more disordered. Obviously, changes of membrane structures shown in Fig. 3 and 4 are quite similar to that shown in Fig. 1 and 2, respectively. This is mainly because increase of spinning time and increase of spinning speed have a similar effect during the depositing process, specifically, both of them would decrease the layer thickness and evaporate the solvent. As for how these two effects resulted in the formation of structures shown in Fig. 3 and 4, our proposed mechanism has been presented above.

To test the validity of our previous explanation on the spinning condition-structure relationship, we prepared two membranes under extreme conditions, e.g., at very high spinning speed and very long spinning time. Structures of the two membranes were shown in Fig. 5 and 6.

It can be found in Fig. 5 that surfaces of the two membranes showed a nodular structure. In Fig. 6, the cross-sections became relatively compacted, no obvious macrovoids can be found. Our explanation to these structures is given below. With very high spinning speed and long spinning time, during spinning, many solvent will evaporate from the deposited layer. The more the solvent evaporated, the higher the layer viscosity became, which, in turn, would slow the subsequent solvent evaporation. When the polymer content increased to a certain value, phase separation would occur to the layer. Since the polymer concentrating speed gradually decreased, thus, it is possible for the polymer molecules to reorient and crystallize. Due to this, it is reasonable to think that the nodular surface structures of these two membranes were mainly caused by the crystallization behavior during the spinning process [20,21]. Moreover, crystallization in the subsequent immersion-precipitation process might also contribute to the formation of these structures.

As shown by Fig. 6(a), the comparatively porous structure indicates that it was the composite result

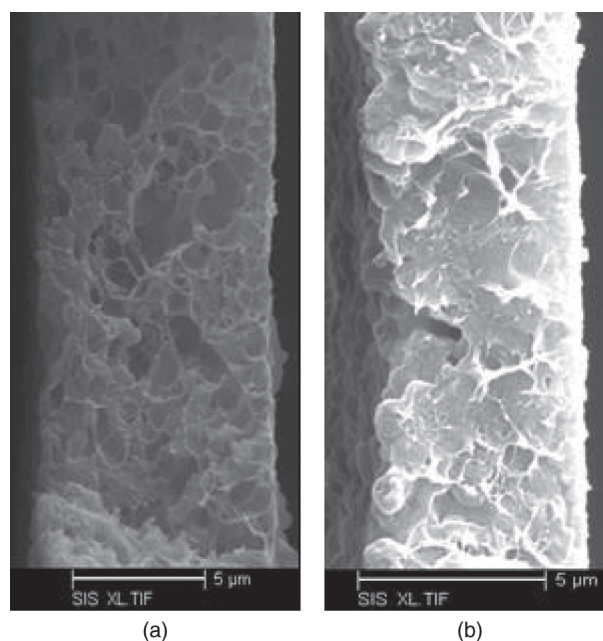


Fig. 6. Cross-section structures of the two membranes shown in Fig. 5.

of solvent evaporation in the spinning process and coagulation of the concentrated solution layer in the immersion-precipitation step. While the compacted structure shown by Fig. 6(b) implies that the evaporation of solvent and solidification of solution layer in the spinning process played a dominating role.

3.3. Flux and rejection measurement

Effects of the spinning time and speed on the filtration property of the membranes were shown in Fig. 7 and 8, respectively.

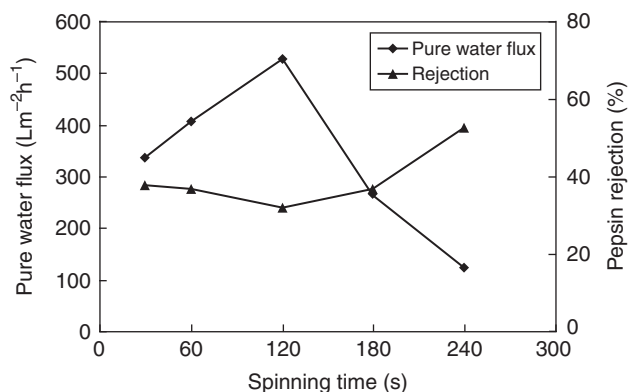


Fig. 7. Effect of spinning time (spinning speed 3000 r/min) on pure water flux and rejection of the membranes.

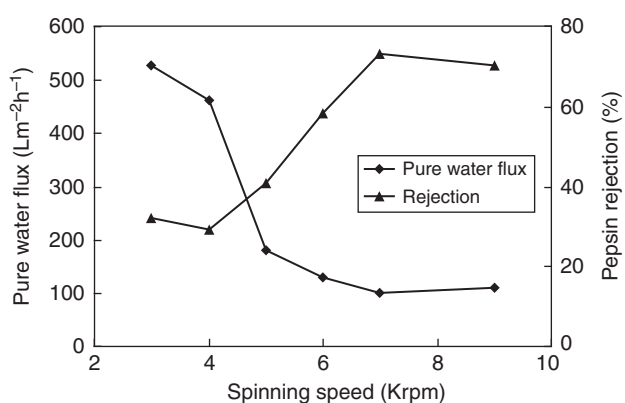


Fig. 8. Effect of spinning speed (spinning time 120s) on pure water flux and rejection of the membranes.

Permeability of a membrane is influenced by its surface, cross-section, and thickness. In Fig. 7, flux of the membranes firstly increased as the spinning time increased from 30s to 120s, then decreased as the spinning time increased from 120s to 240s. Increase of the flux of those membranes with typical macrovoid structures was thought to be mainly caused by the decrease of membrane thickness (Fig. 2(a) and (b)). While decrease of the flux of those membranes with disordered cross-section was thought to be caused by the increasing compaction of membrane cross-section. It is easy to understand that the increasing compaction was caused by the solvent evaporation induced polymer concentration in the spinning process.

Rejection property of the membranes shown in Fig. 7 displayed an inverse trend to that of the flux. This kind of flux-rejection relationship is very general, however, the point is why membrane with more porous surface (Fig. 1) has a higher rejection coefficient and lower flux. The possible answer is given below.

On one hand, those visible pores on membrane surface (Fig. 1(c) and (d)) do not necessarily mean that they are cylindrical and open pores. These pores might end in the dense selective layer, in other words, those membranes with visible pores on surface might have a denser thus more resistant selective layer. On the other hand, the pepsin is about 5 nm in size, so the pores on membrane surface which really determine its passage are not visible on the SEM photos shown in Fig. 1. It is reasonable to think that, from the rejection values shown in Fig. 7, those membranes with big visible pores should have much smaller “effective” pores on membrane surfaces.

In Fig. 8, flux of the membranes decreased as the spinning speed increased from 3 Krpm to 7 Krpm, this should be mainly caused by the solvent evaporation induced structure compaction. However, the reason for the flux difference of the two membranes prepared at 7 and 9 Krpm is not clear. Again, the rejection of these membranes showed an inverse trend to that of the flux.

4. Conclusion

Polymeric membranes were deposited and coagulated using the spinning coating method and immersion-precipitation method, respectively. The effects of spinning speed and time on membrane structure (surface, cross-section, thickness) and property (permeability, rejection) were investigated. The results showed that membranes with smooth, dense, porous, or nodular surface, with macrovoid, disordered, the combination of them, or very dense cross-section all can be formed through proper control on spinning process. Some membranes with porous surface do not necessarily mean that they would possess higher flux.

Acknowledgement

The support from National Natural Science Foundation of China is greatly appreciated (projects' number: 50778049, 50978067).

References

- [1] M. Ulbricht, Advanced functional polymer membranes, *Polymer*, 47 (2006) 2217–2262.
- [2] X.H. Yan, G.J. Liu, M. Dickey and C.G. Willson, Preparation of porous polymer membranes using nano- or micro-pillar arrays as templates, *Polymer*, 45 (2004) 8469–8474.
- [3] D.M. Wang, T.T. Wu, F.C. Lin, J.Y. Hou and J.Y. Lai, A novel method for controlling the surface morphology of polymeric membranes. *J. Membr. Sci.*, 169 (2000) 39–51.
- [4] B.J. Hinds, N. Chopra, T. Rantell, R. Andrews, V. Gavalas and L.G. Bachas, Aligned multiwalled carbon nanotube membranes, *Science*, 303 (2004) 62–65.

- [5] K.B. Jirage, J.C. Hulteen and C.R. Martin, Nanotubule-Based Molecular-Filtration Membranes, *Science*, 278 (1997) 655–658.
- [6] C.A. Smolders, A.J. Reuvers, R.M. Boom and I.M. Wienk, Microstructures in phase-inversion membranes, Part I. Formation of macrovoids, *J. Membr. Sci.*, 73 (1992) 259–275.
- [7] P. Witte, P.J. Dijkstra, J.W.A. van den Berg and J. Feijen, Phase separation processes in polymer solutions in relation to membrane formation, *J. Membr. Sci.*, 117 (1996) 1–31.
- [8] C. Stropnik, V. Musil and M. Brumen, Polymeric membrane formation by wet-phase separation: turbidity and shrinkage phenomena as evidence for the elementary processes, *Polymer*, 41 (2000) 9227–9237.
- [9] C. Stropnik and V. Kaiser, Polymeric membranes preparation by wet phase separation: mechanisms and elementary processes, *Desalination*, 145, (2002) 1–10.
- [10] A.S. Zalusky, R. Olayo-Valles, J.H. Wolf and M.A. Hillmyer, Ordered Nanoporous Polymers from Polystyrene–Polylactide Block Copolymers, *J. Am. Chem. Soc.*, 124 (2002) 12761–12773.
- [11] C. Park, J. Yoon, E.L. Thomas, Enabling Nanotechnology with Self Assembled Block Copolymer Patterns, *Polymer*, 44 (2003) 6725–6760.
- [12] Y. Liu, G.H. Koops and H. Strathmann, Characterization of morphology controlled polyethersulfone hollow fiber membranes by the addition of polyethylene glycol to the dope and bore liquid solution, *J. Membr. Sci.*, 223 (2003) 187–199.
- [13] S.S. Prakash, L.F. Francis and L.E. Scriven, Microstructure evolution in dry–wet cast polysulfone membranes by cryo-SEM: A hypothesis on macrovoid formation, *J. Membr. Sci.*, 313 (2008) 135–157.
- [14] D.M. Vaessen, A.V. McCormick and L.F. Francis, Effects of phase separation on stress development in polymeric coatings, *Polymer*, 43 (2002) 2267–2277.
- [15] Z. Pientka, L. Brožová, M. Bleha and P. Puri, Preparation and characterization of ultrathin polymeric films, *J. Membr. Sci.*, 214 (2003) 157–161.
- [16] C.D. Sheraw, D.J. Gundlach and T.N. Jackson, Spin-on polymer gate dielectric for high performance organic thin-film transistors, *Material Research Society, Mater. Res. Soc. Symp. Proc.*, (2000) 403–408.
- [17] K. Norrman, A. Ghanbari-Siahkali and N.B. Larsen, Studies of spin-coated polymer films, *Annu. Rep. Prog. Chem., Sect. C*, 101 (2005) 174–201.
- [18] M. Yoshikawa, J. Izumi, Y. Kitao, S. Koya and S. Sakamoto, Molecularly Imprinted Polymeric Membranes for Optical Resolution, *J. Membr. Sci.*, (1995) 171–175.
- [19] M. Yoshikawa, T. Ooi and J. Izumi, Alternative molecularly imprinted membranes from a derivative of natural polymer, cellulose acetate, *J. Appl. Polym. Sci.*, 72 (1999) 493–499.
- [20] D.J. Lin, K. Beltsios, T.H. Young, Y.S. Jeng and L.P. Cheng, Strong effect of precursor preparation on the morphology of semicrystalline phase inversion poly(vinylidene fluoride) membranes, *J. Membr. Sci.*, 274 (2006) 64–72.
- [21] L.P. Cheng, Effect of temperature on the formation of microporous PVDF membranes by precipitation from 1-Octanol/DMF/PVDF and Water/DMF/PVDF systems, *Macromolecules*, 32 (1999) 6668–6674.